

See discussions, stats, and author profiles for this publication at: <http://www.researchgate.net/publication/273152477>

Differential Microfluidic Sensor on PCB for Biological Cells Analysis

ARTICLE *in* ELECTROPHORESIS · MARCH 2015

Impact Factor: 3.03 · DOI: 10.1002/elps.201400524 · Source: PubMed

READS

42

9 AUTHORS, INCLUDING:



Jinhong Guo

Nanyang Technological University

30 PUBLICATIONS 48 CITATIONS

SEE PROFILE



Ye Ai

Singapore University of Technology and De...

45 PUBLICATIONS 511 CITATIONS

SEE PROFILE



Yuejun Kang

Nanyang Technological University

90 PUBLICATIONS 976 CITATIONS

SEE PROFILE

Dongyuan Shi¹
Jinhong Guo^{1,2*}
Liang Chen¹
Chuncheng Xia¹
Zhefeng Yu³
Ye Ai²
Chang Ming Li⁴
Yuejun Kang⁵
Zhiming Wang¹

¹Institute of Fundamental and Frontier Sciences, University of Electronic Science and Technology of China, Chengdu, P. R. China

²Pillar of Engineering Product Development, Singapore University of Technology and Design, Singapore, Singapore

³China Aerodynamics Research & Development Center; Mianyang, Sichuan, P. R. China

⁴Institute for Clean Energy and Advanced Materials, Southwest University, Beibei, Chongqing, P. R. China

⁵School of Chemical and Biomedical Engineering, Nanyang Technological University, Singapore, Singapore

Received November 1, 2014

Revised January 22, 2015

Accepted February 4, 2015

Coulter principle based resistive pulse sensor has been demonstrated as a powerful platform to characterize particles or biological cells suspended in liquid electrolytes since it was developed in 1953 [1], which has been widely utilized in biomedical and biomedicine applications such as the analyses of macroparticles [2], detection and enumeration of red/white blood cells [3], circulating tumor cells (CTCs) [4], bacteria [5], viruses [6], and biomolecules [7–9]. Concentration of the target cells or bacteria can help provide vital suggestion for clinical diagnosis. As compared to conventional single pulse sensing method, the proposed dual channel structure can behave better sensitivity since it moderates the noise by differentiating the single channel signal. The translocation of a nonconducting particle through a micro/nanoscale constricting aperture leads to an increase in the electrical resistance of the aperture due to the replacement of conducting

Correspondence: Dr. Ye Ai, Pillar of Engineering Product Development, Singapore University of Technology and Design, Singapore 138682, Singapore

E-mail: aiye@sutd.edu.sg

Abbreviations: CTC, circulating tumor cells; PCB, printed circuit board

Short Communication

Differential microfluidic sensor on printed circuit board for biological cells analysis

Coulter principle based resistive pulse sensor has been demonstrated as an important platform in biological cell detection and enumeration since several decades ago. Recently, the miniaturized micro-Coulter counter has attracted much attention due to its advantages in point of care diagnostics for on chip detection and enumeration of rare cells, such as circulating tumor cells. In this paper, we present a microfluidic cytometer with differential amplifier based on Coulter principle on a SU-8 coated printed circuit board substrate. The electrical current changes induced by the blockage of the microparticles in the sensing aperture are calibrated by polystyrene particles of standard size. Finally, HeLa cells are used to evaluate the performance of the proposed device for enumeration of biological samples. The proposed cytometer is built upon the cheap and widely available printed circuit board substrate and shows its great potential as personalized healthcare monitor.

Keywords:

Circulating tumor cell / Coulter counter / PCB / Personalized healthcare monitor
DOI 10.1002/elps.201400524

solution by the insulating particle in the aperture. This blockage directly results in the significant decrease in the electrical current across the aperture, which is often referred to as the Coulter principle. By analyzing the electrical current pulse induced by blockage of microparticles, this impedance based detection method can implement basic cytometric functions, such as sizing and enumeration of biological cells. In recent years, with rapid development of micro/nanofabrication technology, several microfluidic impedance cytometers have been developed for the increasing needs to address the issues in point of care diagnosis [10–12].

Cancer diagnosis is one of the most important biomedical applications in which microfluidic flow cytometry could have significant and revolutionary impact. Cervical cancer is the third in the common malignant tumors that leads to women death after breast and colorectal cancer in developing countries [13,14]. HeLa cells are the specific circulating tumor cells disseminated from the primary cervical tumors, causing metastases in the cancer patients [15]. CTCs can be detected in the blood circulation of major cancer patients despite of their

*Additional corresponding author: Dr. Jinhong Guo,
E-mail: guojinhong@uestc.edu.cn

Colour Online: See the article online to view Figs. 1–5 in colour.

extremely low concentration. Precise enumeration of CTCs in the circulating blood is believed to be a critical diagnostic parameter for recording disease progression and evaluating the patient response to treatment. However, it is quite challenging to analyze and enumerate the CTCs precisely in the early cancer, which is resulting from the fact that the concentration of CTCs is extremely rare as compared with other blood cells, ~ 1 CTC per million blood cells. Conventional flow cytometry is usually based on optical detection by the utilization of fluorescent staining and immunological attachment based biomarkers, for which the sample pretreatment is both time-consuming and labor intensive. Moreover, some staining reagents are harmful to the cell viability, inducing this process rather difficult to fully recover all the cell events. Although this information loss does not affect the assay of abundant regular blood cells, it is highly deleterious to routine detection of extremely rare cells such as CTCs. On the other hand, microfluidic impedance cytometer provides a robust detection platform and could have great potential to address the current challenges for CTC detection due to their advantages of compactness and portability, small sampling size, ultrahigh sensitivity, and flexible choice of detection modalities [16, 17].

However, many available microfluidic cytometers that implement electrical impedance detection modality require patterning gold electrode probes on a silicon or glass substrate, followed by bonding a microchannel onto the substrate. Obviously it is a nontrivial task to pattern desired gold electrodes on silicon or glass substrate, which requires tedious and expensive surface processing to achieve the desired strong bonding between the gold probes and the substrate material. Hence, this significantly increases the fabrication cost of the microfluidic impedance cytometer and limits its wide application for point of care diagnosis. To address this problem, in this paper, we propose a microfluidic cytometer that is directly built on a cheap printed circuit board (PCB) as substrate, which includes the deposited metal electrodes ready to use and is commercially available. In addition, since dual channel and the corresponding differential amplifier were applied in the proposed chip, the signal to noise can be significantly improved. The microfluidic channel can be integrated on this PCB directly through a simple and fast procedure, providing a highly cost effective platform for detection and enumeration of CTCs.

The structure of the microfluidic cytometer in this paper is composed of dual main channel and dual sensing aperture. As Fig. 1 indicates, two electrodes are deposited on the PCB covered by a thin layer of SU-8 that was spin coated on the PCB. By standard photolithography, only a small portion of every electrode is exposed so that it can fully contact the fluids in the channel. The dimension of the main channel is $800\ \mu\text{m}$ in width and $20\ \mu\text{m}$ in height; the size of the sensing aperture is $20\ \mu\text{m}$ in width and $50\ \mu\text{m}$ in length. The equivalent electric circuit is shown in Fig. 1B. In the following part, the theoretical analysis and numerical modeling of the pulse amplitude is demonstrated.

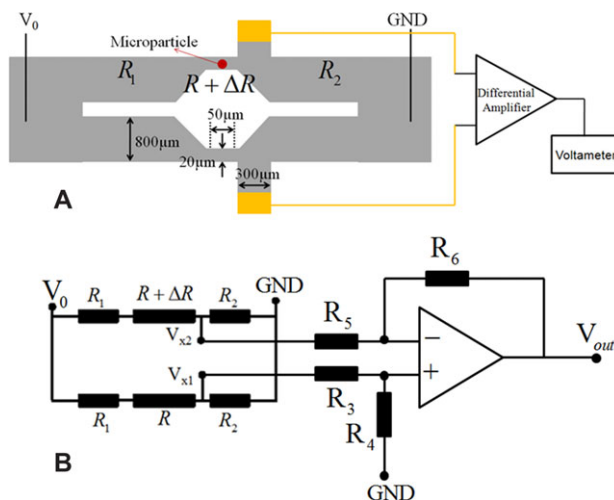


Figure 1. (A) Schematic view of the proposed impedance cytometer. (B) Equivalent electric circuit of the impedance cytometer.

Due to the symmetric structure, only half structure analysis is needed. Since the particle size is much smaller than the channel size in R_1 and R_2 regimes, the electrical impedance modulation of the particle on these two channel sections are negligible. However, when the particle translocates through the narrow sensing aperture R , it will induce a significant modulation on the aperture impedance because its comparable size causes partial blockage of the aperture. We assume ΔR is the resistance change due to the temporary existence of the microparticle in the aperture. The electric current through the aperture without and with a particle inside can be written as:

$$I = \frac{V_0}{R_1 + R_2 + R}; I^* = \frac{V_0}{R_1 + R_2 + R + \Delta R} \quad (1)$$

where V_0 is the total bias across the main channel. The corresponding electrical voltages at the side branch are:

$$V_{x1} = I R_2; V_{x2} = I^* R_2; V_x = V_{x1} - V_{x2}. \quad (2)$$

V_x is the differential voltage of the two sensing nodes. The relative change of branch voltage before and after the particle translocations can be derived from Eqs. (1, and 2):

$$\frac{V_x}{V_{x1}} = \frac{V_{x1} - V_{x2}}{V_{x1}} = \frac{\Delta R}{R_1 + R_2 + R + \Delta R}. \quad (3)$$

Because $\Delta R \ll R_1 + R_2 + R$, the relation between the side branch voltage modulation and the resistance modulation in Eq. (3) can be simplified as:

$$V_x = \frac{V_{x1}}{R_1 + R_2 + R} \Delta R. \quad (4)$$

The resistance modulation induced by a spherical particle inside a channel is also related to the particle size that has been derived by Deblois and Bean [18]. From Eq. (4), the amplitude of the voltage modulation is linearly proportional to

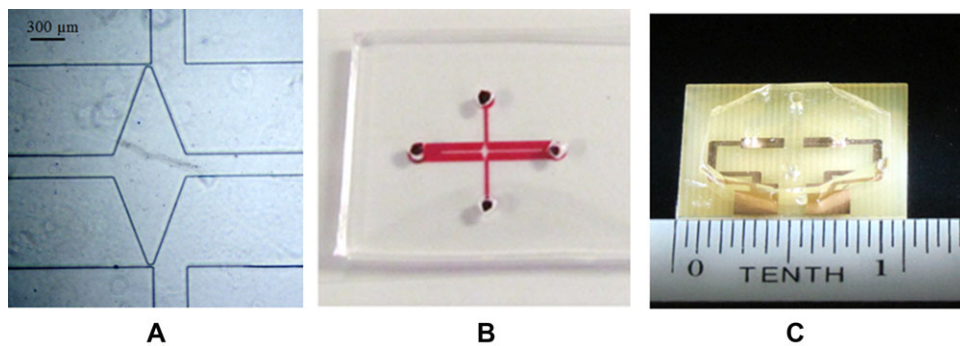


Figure 2. (A) Microscopic image of the dual channel. (B) Microfluidic channel filled with a red ink; (C) Photograph of the proposed PCB-based microfluidic cytometer.

the particle volume [18]. By applying the differential amplifier connecting the dual branch channel, the modulation can be amplified. The equivalent circuit of the proposed microfluidic cytometer is presented in Fig 1B. As long as the ratio of the resistors is tightly matched: $\frac{R_4}{R_3} = \frac{R_6}{R_5}$, the output signal, V_{out} , is approximately to be linearly proportional to the particle volume, written as:

$$V_{out} \approx \frac{R_6}{R_5} \cdot (V_{x1} - V_{x2}) = \frac{R_6}{R_5} \cdot \frac{V_0 R_2}{(R_1 + R_2 + R)^2} \cdot \Delta R \propto V_{particle} \quad (5)$$

The PCB with predeposited Au electrodes was obtained from a commercial supplier (HQPCB, Shen Zhen, China) for a unit price less than US\$2.00. The SU-8 3025 was spun coated on the PCB, soft-baked for 2 min at 65°C and 5 min at 95°C, and exposed to UV light with a photomask. The PCB was then baked on a hot plate for 1 min at 65°C and 2 min at 95°C. After postexposure baking, the master was developed in SU-8 developer solution for 3 min, followed by final baking at 200°C for 10 min. The mold of the PDMS microfluidic channel was fabricated on a silicon wafer, which were cleaned in acetone, methanol, and de-ionized water, and dried on a hot plate for 30 min at 250°C. SU-8 3025 spin-coated on the wafer was soft-baked for 2 min at 65°C and 5 min at 95°C, and exposed to UV light irradiation. The wafer was then baked on a hot plate for 1 min at 65°C and 2 min at 95°C. After post baking, the mold was developed in SU-8 developer solution for 5 min, then was put on the hotplate and baked for 20 min at 250°C. PDMS prepolymer and the curing agent were mixed at a ratio of 10:1, degassed in a vacuum chamber. The mixture was poured on the SU-8 mold and baked in an oven for 2 h at 95°C. PDMS channels were then sliced and peeled off from the SU-8 mold and reservoir holes were punched. The PDMS channel and a clean glass slide were plasma treated for 10 s before they were bonded to form the final chip, as shown in Fig. 2.

HeLa cells (American Type Culture Collection, MD, USA) were cultured in DMEM supplemented with 10% fetal bovine serum (FBS), 1 mM sodium pyruvate, 0.1 mM MEM nonessential amino acids. The cells were grown at 37°C under a 5% CO₂ in a T75 flask. Fig. 3A shows an image of the HeLa cells under a bright-field microscope and Fig. 3B presents an image of the HeLa cells stained in red under a fluorescence microscope.

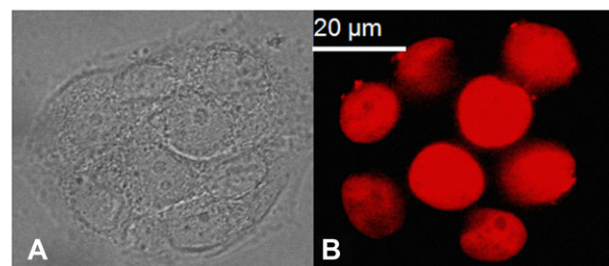


Figure 3. (A) HeLa cells under a bright-field microscope. (B) Stained HeLa cells under a fluorescence microscope.

The dual sensing electrodes were connected to a commercial differential amplifier. Subsequently, the R-C low pass filter was applied to suppress the system noise, and then filtered signal was collected by data acquisition board and experienced the signal processing with MATLAB. During the test, the aluminum Faraday cage was applied to electrically shield the electromagnetic interference. The cells and particles were carried in PBS solution with a concentration of $2 \times 10^3 / \mu\text{L}$ and the flow rate was around 2 $\mu\text{L}/\text{min}$.

Polystyrene particles of various sizes (7, 10, and 16 μm) were introduced into the proposed cytometer to calibrate dynamic detection range. The detected output signals due to the electrical blockage of the microparticles of different size are indicated in Fig. 4A. Once the particle/cell blocks the up channel, V_{x1} will be larger than V_{x2} , which can induce the upward signal. Otherwise the particle/cell blocks the bottom channel, V_{x1} will be smaller than V_{x2} , which can induce the downward signal. In short, upward and downward pulses correspond to the polystyrene particle translocations in the up and bottom sensing apertures, respectively. The amplitude of the pulse mainly depends on the particle size. However, the off-axis of the microparticles is also a minor factor to impact the amplitude, which has been numerically investigated in a previous study [19]. This indicates the detected signal induced by the polystyrene particles of the same size has the perturbations in amplitude. Fig. 4B shows the detected peak amplitude as a function of the particle volume. The average modulation of the electric potential is found to be 0.09 V for 7 μm particles, 0.22 V for 10 μm particles, and 0.9 V for 16 μm particles. The peak amplitude was linearly proportional to the particle volume with a linear regression coefficient $R^2 = 0.9776$. An

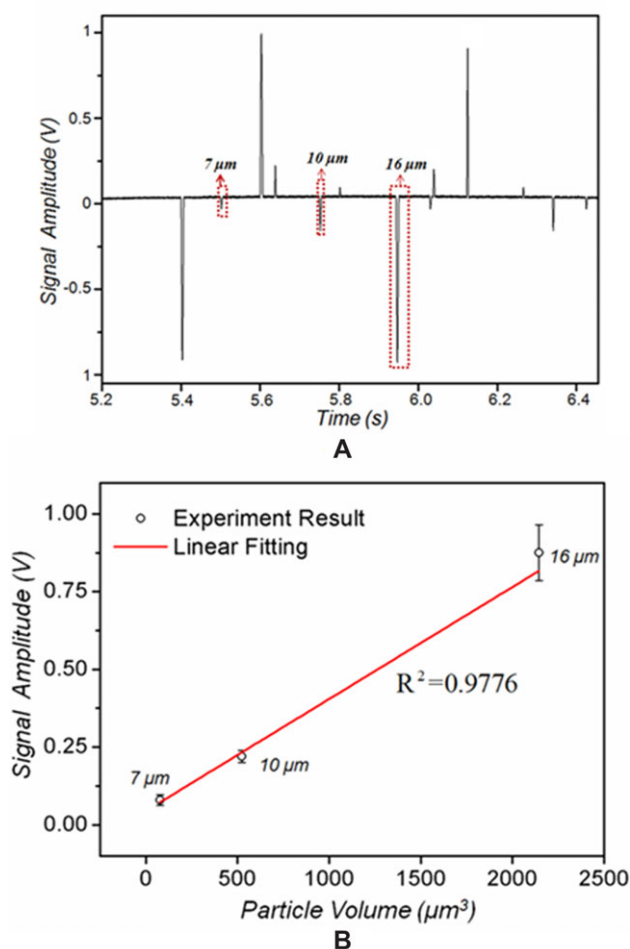


Figure 4. (A) Output signal due to the electrical blockage of 7, 10, and 16 μm polystyrene particles. (B) Output signal peak amplitude as a function of the particle volume.

small increase in particle volume induces significant change in the amplitude of detected signal. From the spikes indicated in Fig. 4, it is easy to distinguish particles of different size.

In order to examine the accuracy of the device for enumeration of actual tumor cells, specific concentrations (Fig. 5A–5C) of HeLa cells were tested by both the proposed chip and a hemocytometer. A series of typical resistance pulse signals for detection of HeLa cells is shown in Fig. 5D. For the output voltage signal monitoring, each up/down spike indicates a CTC cell event and the amplitude of the pulse is proportional to the volume (i.e., size) of the cell. The comparison of both results is shown in Fig. 5E, which demonstrates good accuracy of the developed chip as compared to the commercial cytometer. This study shows that the presented cytometer built on PCB is able to provide reliable platform for cell enumeration, such as analysis of CTCs, which is a promising platform for future point of care diagnosis, especially in the resource-poor developing countries.

In conclusion, in this paper, we demonstrated a PCB-based microfluidic impedance cytometer for detection and

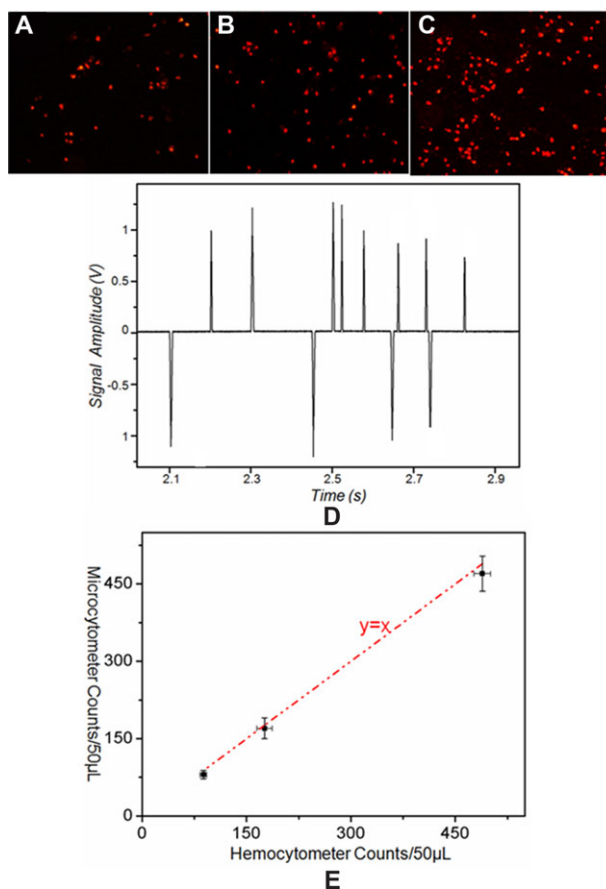


Figure 5. (A–C) Different concentrations of the stained HeLa cells under fluorescence microscope (in the ranges of $1.6 \times 10^3 / \mu\text{L}$, $4 \times 10^3 / \mu\text{L}$, $1 \times 10^4 / \mu\text{L}$, respectively), (D) Continuous record of output signal profiles induced by HeLa cells. (E) Enumeration of HeLa cells by both commercial cytometer and the proposed chip with a good agreement.

enumeration of circulating tumor cells toward the point of care diagnosis. As compared to other available microfluidic impedance cytometers based on functionalized silicon or glass substrates, this proposed microfluidic impedance sensor is simply built upon cheap and widely available PCB, on which the electrodes have been predeposited and are ready to use. Therefore, this unique approach for fast interfacing the microfluidic cytometry chip with the external measurement system provides a highly cost-effective platform for rapid point of care detection and enumeration of rare cells.

This research is supported by a seed grant from Institute of Fundamental and Frontier Science at University of Electronic Science and Technology of China awarded to J.Guo. and SUTD-MIT International Design Center IDG11300101 awarded to Y.A.

The authors have declared no conflict of interest.

References

- [1] Coulter, W. H., *US Patent* (1953) No 2656508.

- [2] Jagtiani, A. V., Zhe, J., Hu, J., Carletta, J., *Meas. Sci. Technol.* 2006, 17, 1706–1714.
- [3] Asghar, W., Wan, Y., Ilyas, A., Bachoo, R., Kim, Y. T., Iqbal, S. M., *Lab Chip* 2012, 12, 345–2352.
- [4] Guo, J., Li, C.M., Kang, Y., *Biomed. Microdevices* 2014, 16, 681–686.
- [5] Guo, J., Li, H., Chen, Y., Kang, Y., *IEEE Sens. J.* 2014, 14, 2112–2117.
- [6] Jeffrey, I. Z., *Semin. Thromb. Hemost.* 2010, 36, 819–823.
- [7] Lorenz, J. S., Oliver, O., Catalin, C., Joanne, G., Ulrich, F. K., *Nano Lett.* 2010, 10, 2493–2497.
- [8] Bayley, H., Martin, C. R., *Chem. Rev.* 2000, 100, 2575–2594.
- [9] Dekker, C., *Nat. Nanotechnol.* 2007, 2, 209–215.
- [10] Guo, J., Lei, W., Ma, X., Xue, P., Chen, Y., Kang, Y., *IEEE Trans. Biomed. Circuits Syst.* 2014, 8, 35–41.
- [11] Wang, Y. N., Kang, Y., Xu, D., Chon, C. H., Barnett, L., Kalams, S. A., Li, D., *Lab Chip* 2008, 8, 309–315.
- [12] Zheng, Y., Nguyen, J., Wang, C., Sun, Y., *Lab Chip* 2013, 16, 3275–83.
- [13] Bosch¹, F. X., Lorincz², A., Muñoz³, N., Meijer⁴, C. J. L. M., Shah⁵, K. V., *J. Clin. Pathol.* 2002, 55, 244–265.
- [14] Kohn, E.C., Liotta, L.A., *Cancer Res.* 1995, 55, 1856–1862.
- [15] Schwarz, E., Freese, U. K., Gissmann, L., Mayer, W., Roggenbuck, B., Stremmlau, A., Hausen, H. Z., *Nature* 1985, 314, 111–114.
- [16] Guo, J., Pui, T. S., Rahman, A.R.R., Kang, Y., *Electrophoresis* 2013, 34, 417–424.
- [17] Watkins, N., Venkatesan, B. M., Toner, M., Rodriguez, W., Bashir, R., *Lab Chip* 2009, 22, 3177–3184.
- [18] DeBlois, R. W., Bean, C. P., Wesley, R. K. A., *J. Colloid Interface Sci.* 1977, 61, 323–335.
- [19] Qin, Z., Zhe, J., Wang, Meas., G. X., *Sci. Technol.* 2011, 22, 045804.